separations

MDPI

Article

Antitumor Potential of Green Synthesized ZnONPs Using Root Extract of *Withania somnifera* against Human Breast Cancer Cell Line

Kollur Shiva Prasad [1,*], Shashanka K Prasad [2], Ravindra Veerapur [3], Ghada Lamraoui [4], Ashwini Prasad [5], M. N. Nagendra Prasad [6], Sandeep Kumar Singh [7], Najat Marraiki [8], Asad Syed [8,*] and Chandan Shivamallu [2,*]

1 Department of Sciences, Amrita School of Arts and Sciences, Amrita Vishwa Vidyapeetham, Mysuru Campus, Mysuru, Karnataka 570026, India
2 Department of Biotechnology and Bioinformatics, School of Life Sciences, JSS Academy of Higher Education and Research, Mysuru, Karnataka 570015, India; shashankaprasad@jssuni.edu.in
3 Department of Metallurgy and Materials Engineering, Malawi Institute of Technology, Malawi University of Science and Technology, P.O. Box 5916, Limbe, Malawi; rveerapur@must.ac.mw
4 Nature and Life Sciences, Earth and Universe Sciences, University of Tlemcen, Tlemcen, Algeria; lamraouig@gmail.com
5 Department of Microbiology and Tissue Culture, School of Life Sciences, JSS Academy of Higher Education and Research, Mysuru, Karnataka 570015, India; ashwinip@jssuni.edu.in
6 Department of Biotechnology, JSS Science and Technolgy University, Mysuru, Karnataka 570004, India; mnnagendraprasad@sjce.ac.in
7 Indian Scientific Education and Technology (ISET) Foundation, Lucknow 226002, India; sandeeps.bhu@gmail.com
8 Department of Botany and Microbiology, College of Science, King Saud University, P.O. Box 2455, Riyadh 11451, Saudi Arabia; najat@ksu.edu.sa
* Correspondence: shivachemist@gmail.com (K.S.P.); assyed@ksu.edu.sa (A.S.); chandans@jssuni.edu.in (C.S.)

Abstract: Herein we report the synthesis of zinc oxide nanoparticles (ZnONPs) using *Withania somnifera* root extract (WSE) as an effective chelating agent. The microscopic techniques viz., X-ray diffraction analysis (XRD), scanning electron microscopy (SEM), transmission electron microscopy (TEM), high-resolution transmission electron microscopy (HRTEM), and selected area electron diffraction (SAED) were employed to analyze the as-obtained ZnONPs. The crystalline planes observed from the XRD pattern agrees with the hexagonal wurtzite structure of the as-prepared ZnONPs. The aggregations and agglomerations observed in the SEM images indicated that the size of the as-prepared ZnONPs was between 30 and 43 nm. The interplanar distance between the lattice fringes observed in the HRTEM image was found to be 0.253 nm, which is in good agreement with the (100) plane obtained in the XRD pattern. Furthermore, the anti-breast cancer cytotoxic evaluation was carried out using the MCF-7 cell line, and the results showed significant cytotoxic effects in a dose-dependent manner.

Keywords: biosynthesis; *Withania somnifera*; ZnONPs; cytotoxicity

Citation: Prasad, K.S.; Prasad, S.K; Veerapur, R.; Lamraoui, G.; Prasad, A.; Prasad, M.N.N.; Singh, S.K.; Marraiki, N.; Syed, A.; Shivamallu, C. Antitumor Potential of Green Synthesized ZnONPs Using Root Extract of *Withania somnifera* against Human Breast Cancer Cell Line. *Separations* **2021**, *8*, 8. https://doi.org/10.3390/separations8010008

Received: 3 December 2020
Accepted: 12 January 2021
Published: 18 January 2021

1. Introduction

Withania somnifera (L.) Dunal, commonly called winter cherry/Indian ginseng (English) or *ashwagandha* (Sanskrit) has been widely used in traditional medicinal practices such as Ayurveda medicinal applications ranging from boosting immunity to increasing longevity [1,2]. Growing about two feet long into a gray, erect, and hairy evergreen shrub, *W. somnifera* is primarily found in the tropical regions of the Americas, Mediterranean, Africa, and India [3]. The biomedical significance of *W. somnifera* plant organs is attributed to the presence of phytochemicals such as lactones and alkaloids [1]. Yang et al. (2013) suggested the use of *W. somnifera* as an alternative therapy to prevent breast cancer metastasis if used on a long-term basis. Such advice was based on an in vivo observation in

rats, where the root extract of *W. somnifera* was able to inhibit the metastasis with minimal adversity to the animal [4]. In a study conducted by Roy et al. (2013), withferin A, a steroidal lactone isolated from *W. somnifera*, demonstrated anti-tumorigenic potential against prostate tumors by inducing cytotoxicity via the metabolic inactivation of a Cdc2-mediated mitotic catastrophe [5]. Similar conclusions were drawn in another study where withanone, a *W. somnifera* alkaloid, disrupted the mitotic procedure by inhibiting survivin, a protein essential for cancer cell survival and proliferation, by binding at the BIR5 binding site of the protein [6]. Winters (2006) concluded that the plant constituted various potent anticancer agents that showed antioxidant and anti-inflammatory abilities without influencing the therapeutic effects of the traditional antineoplastic agents [7].

Meanwhile, ZnONPs, a versatile drug delivery tool, have recently been reported to possess significant tumoricidal activity via reactive oxygen species (ROS) generation or caspase-8 and p53 [8–11]. However, a better understanding of the mechanistic mode and the resultant cellular consequences is essential. Although the metal oxide is considered by the USFDA to be a "generally recognized as safe" (GRAS) substance [12], such a categorization typically applies to substances larger than a micron. Hence it may be deemed necessary to evaluate the cytotoxicity of the same in both in vitro and in vivo systems. In this study, we tried to re-evaluate the cytotoxic efficacy of ZnONPs functionalized with *W. somnifera* root extract (WSE) in the breast cancer cell line (MCF-7).

2. Materials and Methods

Anhydrous zinc acetate [$Zn(OAc)_2$] obtained from S.D. Fine Chemicals Ltd. (Mumbai, MH, India), solvents were procured from Merck chemical suppliers (RD Chem, Mumbai, MH, India). Commercial ZnONPs (20–30 nm) were procured from Alfa Aesar (Austin, TX, USA). Triple distilled water was used throughout the experiments (ELGA RO water purifier, Elga Veolia, Lane End, UK). Infrared spectra were recorded using the PerkinElmer spectrometer (PerkinElmer, Salt Lake, OH, USA) version 10.03.09 (KBr pellet technique). The electronic absorption spectra were recorded on a PerkinElmer Lambda 750 UV-Visible spectrophotometer (PerkinElmer, Salt Lake, OH, USA). Powder X-ray diffraction patterns was obtained on a Bruker X-ray diffractometer using Cu Kα (1.5406 Å) radiation (Bruker, Karlsruhe, Germany). Scanning electron microscopy (SEM) images were recorded on Zeiss microscope (Carl Zeiss, White Plains, NY, USA). Transmission electron microscopy (TEM) images and selected area diffraction patterns were measured using a JEOL 2100F FEG microscope at 200 kV after casting a drop of ZnONP dispersion in ethanol over a Cu grid (Jeol, Akishima, Tokyo, Japan).

2.1. Plant Material Collection and Extraction

Fresh roots of *Withania somnifera* were collected from Mysuru Gaya Local Area, Karnataka State (geographical coordinates: 12.319458, 76.6940601, 15.79z). The plant root authentication was done by a botanist of the Department of Botany, University of Mysore, Karnataka, India. The specimen voucher number WS201 was given to the selected plant and was deposited at the herbarium of the JSS Academy of Higher Education and Research. The root pieces were washed properly with deionized water, shade dried, and then minced into a coarse powder using a blender. The dried plant material (52.8 g of the whole mass) was extracted using water as a solvent by a soxhlet apparatus at 60 °C (1:4 *w*/*v*). The extract thus obtained was filtered and dried in a hot air oven to yield the crude extract of the *Withania somnifera* root.

2.2. Preparation of ZnONPs

The aqueous root extract of *Withania somnifera* (0.32 g dissolved in 15 mL deionized water) was added to an aqueous solution of anhydrous zinc acetate (1 mM, 1.83 g) in 25 mL of deionized water and the mixture was stirred for 4 h. The formation of a pale yellow color indicated the formation of WSE + ZnONPs from the above mixture. Furthermore, this observation also confirmed the involvement of the functional groups viz., hydroxyl,

amine, carbonyl groups, etc., towards the zinc ion coordination. The material thus obtained was washed with ethyl alcohol followed by acetone. The product obtained was dried at 100 °C for 10 h.

2.3. In Vitro Anti-Breast Cancer Activity Evaluation

The cell line was obtained from Azyme Biosciences Pvt. Ltd., Bengaluru, India, who maintain the ATCC cell cultures. The anti-breast cancer cytotoxic effects of WSE, commercially available ZnONPs, and WSE + ZnONPs (10 µg) were determined on MCF-7 cell lines purchased from American Type Culture Collection (ATCC), Manassas, VA, USA, using an MTT (3-(4,5-dimethylthiazol-2-yl)-2,5-diphenyltetrazolium bromide) assay. The MCF-7 cells were cultured in Dulbecco's Modified Eagle Medium (DMEM) containing 10% fetal bovine serum (FBS), 100 IU/mL penicillin, and 100 µg/mL streptomycin in 5% CO_2 at 37 °C until confluent. Trypsinization was carried out using a 0.05% trypsin-EDTA solution for the cellular viability to be checked using a haemocytometer. A total of 100 µL of the media-diluted cell suspensions containing 10,000 cells/well were plated and incubated in 5% CO_2 at 37 °C until confluence. The cells were treated with 2.5, 5, 10, 20, and 40 µg/mL concentrations of WSE, ZnONPs, and WSE + ZnONPs (10 µg).

2.4. Measurement of % Inhibition Using MTT Assay

The MTT assay was performed as previously performed according to Denizot and Lang (1986) [13] to check for % inhibition. Upon treatment for 24 h, the cells were fixed using an MTT reagent (5 mg/mL) to each well and incubated at 37 °C for 1 h, followed by centrifugation at 3000 rpm for 5 min. Excess dye was removed from the plates by washing using distilled water and kept for air drying. Following this, 100 µL of DMSO was added to solubilize the crystal and optical density was read at 570 nm. The percentage inhibition was calculated using Formula (1), mentioned below:

$$\% \, inhibition = 100 - \left[\frac{OD \, of \, sample - OD \, of \, blank}{OD \, of control - OD \, of \, blank} \right] \times 100 \quad (1)$$

The observations made were represented graphically and statistically using the Prism 8 statistical analysis tool (GraphPad Software, San Diego, CA, USA).

3. Results and Discussion

The ZnONP formation was visually noticed during the biosynthesis, where the color of the solution during the reaction changed from greenish yellow to pale yellow after adding the WSE to an aqueous solution of zinc acetate.

3.1. Powder X-ray Diffraction Analysis

The crystallinity and the phase distribution of the as-prepared ZnONPs were determined by analyzing the powder XRD spectrum, as depicted in Figure 1. The positions and the intensities inferred that the as-obtained ZnONPs were in their pure phase, without any diffraction peaks from impurities [14]. Furthermore, the results suggest that the h k l values observed at (100), (002), (101), (102), (110), (103), (200), (112), (201), and (004) belonged to the crystalline planes, which were matched with the standard JCPDS data of 36-1451, which agreed with the hexagonal wurtzite structure [15]. Furthermore, the average particle size of the as-prepared ZnONPs was said to be 32 nm, which was calculated (using FWHM) by Scherrer's formula, $D = k\lambda/\beta\cos\theta$ [16].

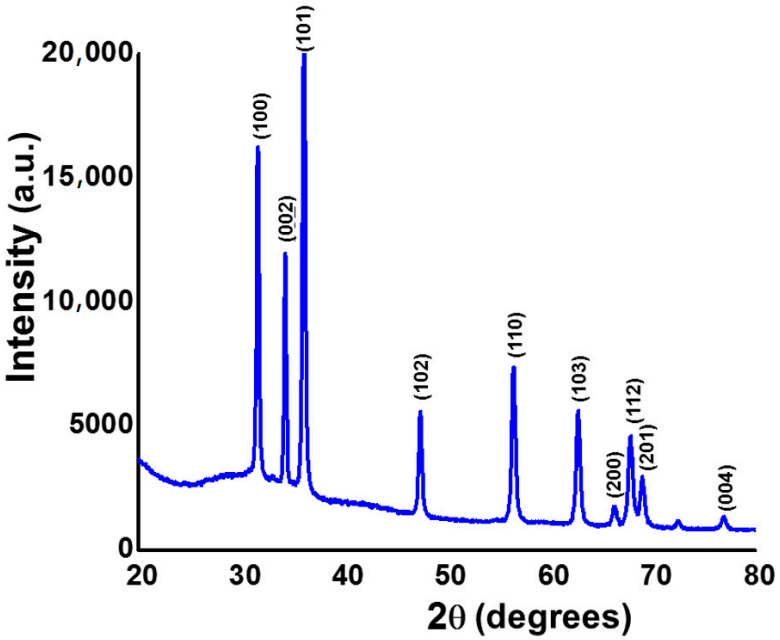

Figure 1. The intensity vs. 2θ profile obtained for the ZnONPs prepared using aqueous root extract of *Withania somnifera*, suggesting that this pattern clearly belongs to the hexagonal crystal structure (JCPDS data of 36-1451).

3.2. Electronic Absorption Spectral Analysis

The UV–vis absorption spectra revealed a characteristic maximum absorbance at 328 nm corresponding to a bandgap of 3.28 eV (Figure 2), which could be due to intrinsic bandgap absorption of ZnO and electron transitions from the valence band to the conduction band. The bandgap (E_g) of the bulk ZnO material (E_g = 3.45148 eV) was greater than the estimated bandgap of the as-synthesized ZnONPs due to the effective size of the nanoparticles. The peak noticed in the absorption spectra imply that the particles were nanosized with narrow particle size distribution. The peak was shifted away from the origin when compared to the bulk, indicating the redshift was due to quantum size effects. In addition, we also noticed a hump at 408 nm, which was due to transitions between Z*ni* to the valence band [17].

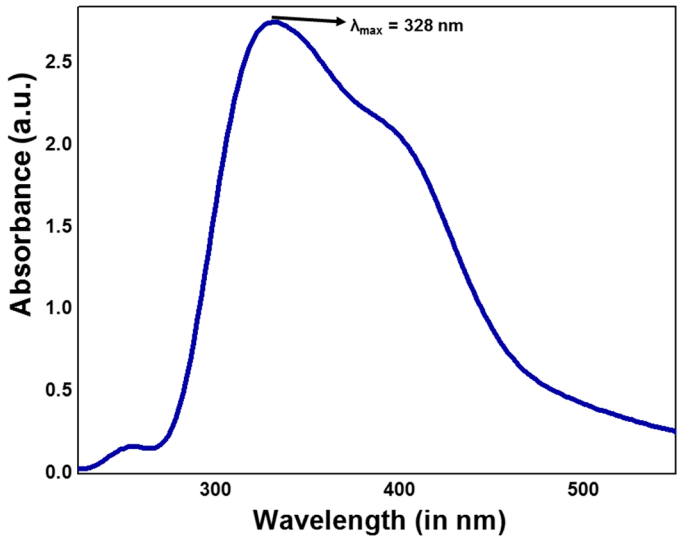

Figure 2. UV–visible spectrum of the as-prepared ZnONPs, measured in the dispersed form in ethanol solution showing λ_{max} = 328 nm.

3.3. Infrared Spectral Analysis

The FT-IR spectra of the leaf extract (Figure 3a) and ZnONPs prepared using the root extract of *Withania somnifera* (Figure 3b) revealed that their formation was through chelation of certain functional groups present in the root extract of the aforementioned plant. The bands observed at 3413 cm^{-1} in the root extract were disappeared in the case of the ZnONPs, demonstrating the involvement of hydroxyl groups present in the *Withania somnifera*. Furthermore, the stretching vibrations in the WSE noticed at 2898 and 1693 cm^{-1} were assigned to the C-H and C=O vibrations, which were blue-shifted in the as-prepared ZnONPs, indicating their participation in the formation of nanostructures. Furthermore, the weak bands observed at 453 cm^{-1} revealed the Zn-O stretching, confirming the formation of ZnONPs. Thus, the above observations confirm the role of phytomaterial in the production of ZnONPs [17].

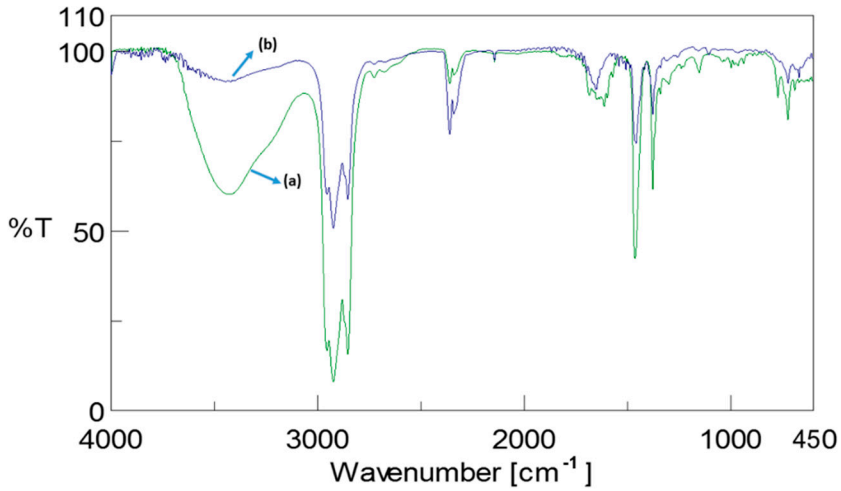

Figure 3. The overlay of FT-IR spectra of (**a**) root extract of *W.sominfera* and (**b**) as-prepared ZnONPs depicting the involvement of various functional groups in their formation.

3.4. Scanning Electron Microscopy (SEM) Analysis

The SEM images of the as-prepared ZnONPs are shown in Figure 4. The SEM results revealed that the prepared nanostructures had an average diameter of between 30 and 43 nm. Further, the aggregations and agglomerations observed in the SEM images were due to the presence of debris from WSE that was use in the preparation process.

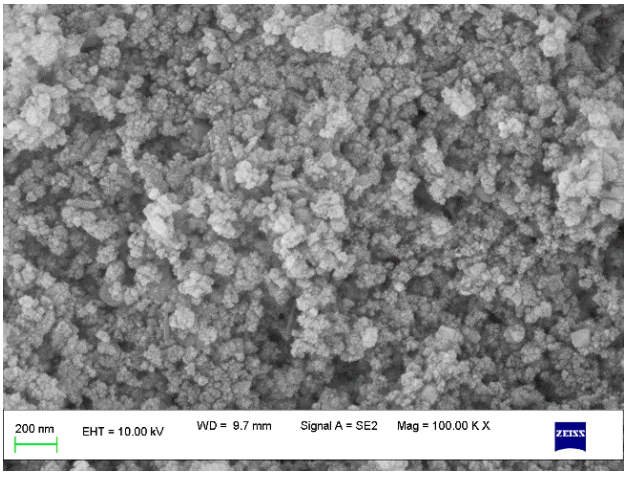

Figure 4. SEM images of ZnONPs synthesized using *Withania somenifera* root extract.

3.5. Transmission Electron Microscopy (TEM) Analysis

The TEM images of the as-prepared ZnONPs are manifested in Figure 5a. It can be seen from the TEM results that as-prepared ZnONPs unveiled a mostly polyhedron shape with a few globular particles ranging from 30 to 45 nm. Furthermore, it can be clearly seen from the TEM image that the presence of dark shadows, which were due to the secondary materials, was mainly from the plant source used for the preparation of ZnONPs [18]. In addition, the interplanar distance between the lattice fringes was found to be 0.253 nm, which was in good agreement with the (100) and (101) planes obtained in the XRD pattern. Furthermore, the SAED concentric circles (inset Figure 5b) endorsed the corresponding (101) and (002) planes.

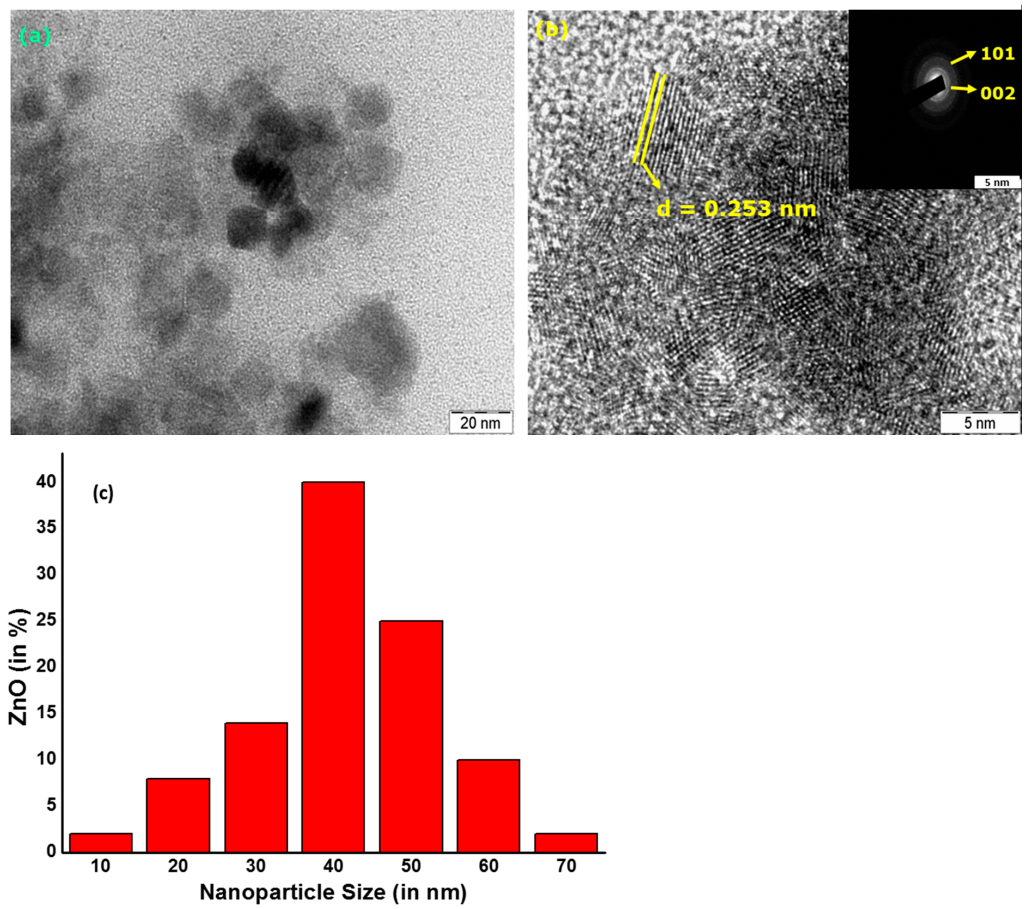

Figure 5. (**a**) TEM image and (**b**) HRTEM showing the SAED (inset) and (**c**) a histogram revealing the size distribution of the as-obtained ZnONPs.

3.6. Cytotoxicity of As-Obtained ZnONPs on Breast Cancer MCF-7 Cell Line

Although all the treatment groups, involving 2.5, 5, 10, 20, and 40 µg/mL concentrations of WSE, commercially available ZnONPs, and WSE + ZnONPs (10 µg), showed dose-dependent anti-breast cancer activity on the MCF-7 cell lines, the cytotoxicity of ZnONPs, although statistically significant, was lower when compared to that of WSE. The IC50 value of the commercially available ZnONPs on MCF-7 cells was calculated to be as high as 13.65 µg/mL. Meanwhile, the WSE showed significant anti-proliferative potential against the breast cancer cells even in small doses. The IC50 value of WSE was found to be 9.014 µg/mL. Notwithstanding, the ZnONP bioproduct obtained from 10 µg of WSE showed a greater antiproliferative effect on the MCF-7 cells with an IC50 value of 6.484 µg/mL.

The current study gains importance from the fact that there has been a drastic shift towards the use of nanoparticles in mediating therapeutic drug deliveries. ZnONPs have

gained importance in this regard. However, studies have highlighted the promiscuity of these nanoparticles, whose bioaccumulation into the ecosystem may be exponentially hazardous because their interactions with the host immune system is as yet ambiguous [18]. Although regulations suggest that the ZnONPs are GRAS, various studies argue that metal oxide nanoparticles are capable of inducing toll-like receptor- (TLR) mediated inflammatory responses apart from depleting the glutathione (GSH) levels, while subsequently acting as a pro-oxidant immunotoxic agent [17,19–23]. In addition, ZnONPs are reported to modulate the macrophage response to diseased conditions [20]. Kumar et al. (2019) suggested that the use of *W. somnifera* extract as a chemoprotective agent against ZnONPs induced in vivo toxicity. Furthermore, it was concluded that the plant extract as well as the phytocompound Withaferin A successfully inhibited ZnONP toxicity and thereby enhanced the immune response of phagocytic macrophages [24]. Likewise, the current study indicates that the ZnONPs prepared using *W. somnifera* root extract showed greater anticancer activity with no adverse effect on the host immune system (Figure 6).

(**a**)

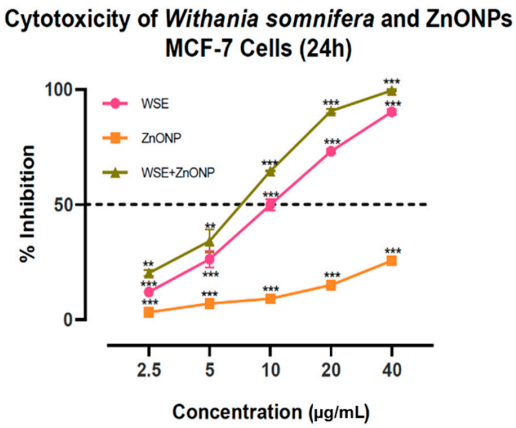

(**b**)

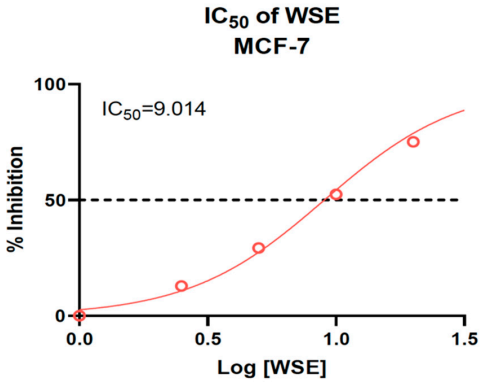

(**c**)

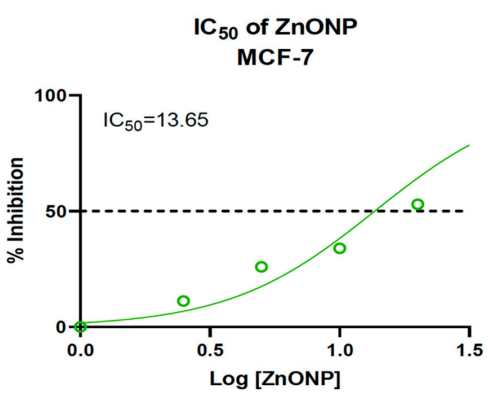

Figure 6. *Cont.*

(**d**)

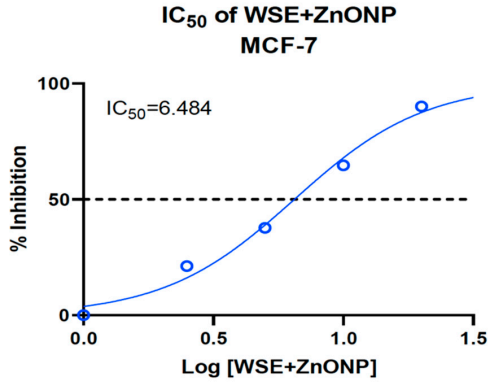

Figure 6. As-prepared ZnONPs using WSE reduced the IC50 value on MCF-7 breast cancer cell lines. (**a**) A comparative graphical representation of the percentage inhibition of the MCF-7 cells by the test samples and (**b**–**d**) individual IC50 calculations for each treatment. n = 3, mean ± SEM, *p* value of <0.05 was considered to be significant, ** *p* = < 0.002, *** *p* = < 0.001, *ns* = not significant.

4. Conclusions

To sum up, ZnONPs were synthesized through a facile and environmentally benign pathway using aqueous *W. somnifera* root extract. The powder XRD pattern confirmed the hexagonal wurtzite structure for the synthesized nanostructures. An absorption maximum observed in the UV–visible absorption studies at 328 nm corresponded to intrinsic bandgap absorption. The SEM studies suggested that the size of as-obtained ZnONPs ranged from 30 to 43 nm, and from TEM images, the interplanar distance found between the lattice fringes was about 0.253 nm, which affirmed the (100) plane obtained in the XRD pattern. Furthermore, it can be concluded that the ZnONPs prepared using *W. somnifera* root extract showed greater anticancer activity compared to the individual treatments of WSE as well as commercially available ZnONPs, while possibly having no adverse effect on the host immune system. This thereby suggests a viable modification in the current therapeutic practices involving metal nanoparticles.

Author Contributions: Conceptualization, K.S.P. and R.V.; methodology, K.S.P.; software, S.K.P., A.P. and M.N.N.P.; validation, S.K.S. and R.V.; formal analysis, K.S.P. and C.S. investigation, K.S.P.; A.S. and N.M; resources, C.S.; data curation, S.K.P. and A.P; writing—original draft preparation, K.S.P., S.K.P., R.V. and C.S.; writing—review and editing, K.S.P.; S.K.P. and R.V.; visualization, S.K.S. and G.L.; supervision, K.S.P.; project administration, C.S. and A.S.; funding acquisition, A.S. and N.M. All authors have read and agreed to the published version of the manuscript.

Funding: The authors extend their appreciation to the researchers supporting project number (RSP-2020/201) King Saud University, Riyadh, Saudi Arabia.

Data Availability Statement: Data available on request due to restrictions.

Acknowledgments: The authors thank the Director, IOE, University of Mysore, Mysuru for the analytical facilities. K.S.P. thankfully acknowledges the Director, Amrita Vishwa Vidyapeetham, Mysuru campus for the infrastructure support. S.K.P. and C.S. acknowledge the support and infrastructure provided by the JSS Academy of Higher Education and Research (JSSAHER), Mysuru, India. The authors extend their appreciation to the researchers supporting project number (RSP-2020/201) King Saud University, Riyadh, Saudi Arabia.

Conflicts of Interest: There is no conflict of interest to declare.

Abbreviations

ZnONPs—zinc oxide nanoparticles; WSE—*Withinia somenifera* root extract; XRD—X-ray diffraction analysis; SEM—scanning electron microscopy; TEM—transmission electron microscopy; HRTEM—high-resolution transmission electron microscopy; SAED—selected area electron diffraction; GRAS—generally recognized as safe; FDA—Food and Drug Administration; FBS—fetal bovine serum; ATCC—

American Type Culture Collection; MTT—(3-(4,5-dimethylthiazol-2-yl)-2,5-diphenyltetrazolium bromide); DMEM—Dulbecco's Modified Eagle Medium.

References

1. Rai, M.; Jogee, P.S.; Agarkar, G.; dos Santos, C.A. Anticancer activities of Withania somnifera: Current research, formulations, and fu-ture perspectives. *Pharm. Biol.* **2016**, *54*, 189–197. [CrossRef] [PubMed]
2. Bhattacharya, S.; Muruganandam, A. Adaptogenic activity of Withania somnifera: An experimental study using a rat model of chronic stress. *Pharmacol. Biochem. Behav.* **2003**, *75*, 547–555. [CrossRef]
3. Khazal, K.F.; Samuel, T.; Hill, N.L.; Grubbs, C.J. Effect of an extract of Withania somnifera root on estrogen receptor-positive mammary carcinomas. *Anticancer Res.* **2013**, *33*, 1519–1523.
4. Yang, Z.; García, A.; Xu, S.; Powell, R.R.; Vertino, P.M.; Singh, S.; Marcus, A.I. Withania somnifera Root Extract Inhibits Mammary Cancer Metastasis and Epithelial to Mesenchymal Transition. *PLoS ONE* **2013**, *8*, e75069. [CrossRef] [PubMed]
5. Roy, R.V.; Suman, S.; Das, T.P.; Luevano, J.E.; Damodaran, C. Withaferin A, a Steroidal Lactone from Withania somnifera, Induces Mitotic Catastrophe and Growth Arrest in Prostate Cancer Cells. *J. Nat. Prod.* **2013**, *76*, 1909–1915. [CrossRef] [PubMed]
6. Wadegaonkar, V.; Wadegaonkar, P. Withanone as an inhibitor of survivin: A potential drug candidate for cancer therapy. *J. Biotechnol.* **2013**, *168*, 229–233. [CrossRef]
7. Winters, M. Ancient medicine, modern use: Withania somnifera and its potential role in integrative oncology. *Altern. Med. Rev. A J. Clin. Ther.* **2006**, *11*, 269–277.
8. Tanino, R.; Amano, Y.; Tong, X.; Sun, R.; Tsubata, Y.; Harada, M.; Fujita, Y.; Isobe, T. Anticancer Activity of ZnO Nanoparticles against Human Small-Cell Lung Cancer in an Orthotopic Mouse Model. *Mol. Cancer Ther.* **2019**, *19*, 502–512. [CrossRef]
9. Bisht, G.; Rayamajhi, S. ZnO Nanoparticles: A Promising Anticancer Agent. *Nanobiomedicine* **2016**, *3*, 9. [CrossRef]
10. Rasmussen, J.W.; Martinez, E.; Louka, P.; Wingett, D.G. Zinc oxide nanoparticles for selective destruction of tumor cells and po-tential for drug delivery applications. *Expert Opin. Drug Deliv.* **2010**, *7*, 1063–1077. [CrossRef]
11. Kadhem, H.A.; Ibraheem, S.A.; Jabir, M.S.; Kadhim, A.A.; Taqi, Z.J.; Florin, M.D. Zinc Oxide Nanoparticles Induces Apoptosis in Human Breast Cancer Cells via Caspase-8 and P53 Pathway. *Nano Biomed. Eng.* **2019**, *11*, 35–43. [CrossRef]
12. *Food for Human Consumption—Substances Generally Recognized as Safe*; 21CFR182.8991; 2019. Available online: https://www.accessdata.fda.gov/scripts/cdrh/cfdocs/cfcfr/CFRSearch.cfm?fr=182.8991 (accessed on 17 January 2021).
13. Denizot, F.; Lang, R. Rapid colorimetric assay for cell growth and survival. Modifications to the tetrazolium dye procedure giving improved sensitivity and reliability. *J. Immunol. Methods* **1986**, *89*, 271–277. [CrossRef]
14. Azizi, S.; Ahmad, M.B.; Namvar, F.; Mohamad, R. Green biosynthesis and characterization of zinc oxide nanoparticles using brown marine macroalga Sargassum muticum aqueous extract. *Mater. Lett.* **2014**, *116*, 275–277. [CrossRef]
15. Hussain, A.; Oves, M.; Alajmi, M.F.; Hussain, I.; Amir, S.; Ahmed, J.; Rehman, M.T.; El-Seedi, H.R.; Ali, I. Biogenesis of ZnO nanoparticles using Pandanus odorif-er leaf extract: Anticancer and antimicrobial activities. *RSC Adv.* **2019**, *9*, 15357–15369. [CrossRef]
16. Elango, G.; Roopan, S.M.; Dhamodaran, K.I.; Elumalai, K.; Al-Dhabi, N.A.; Arasu, M.V. Spectroscopic investigation of biosynthesized nickel nanoparticles and its larvicidal, pesticidal activities. *J. Photochem. Photobiol. B Biol.* **2016**, *162*, 162–167. [CrossRef] [PubMed]
17. Al-Dhabi, N.A.; Arasu, M.V. Environmentally-Friendly Green Approach for the Production of Zinc Oxide Nanoparticles and Their Anti-Fungal, Ovicidal, and Larvicidal Properties. *Nanomaterials* **2018**, *8*, 500. [CrossRef] [PubMed]
18. Sahu, D.; Kannan, G.M.; Vijayaraghavan, R.; Anand, T.; Khanum, F. Nanosized Zinc Oxide Induces Toxicity in Human Lung Cells. *ISRN Toxicol.* **2013**, *2013*, 1–8. [CrossRef]
19. Kollur, S.P.; Prasad, S.K.; Ansari, M.A.; Alzohairy, M.A.; Alomary, M.N.; Alyahya, S.; Srinivasa, C.; Murali, M.; Ankegowda, V.M.; Shivamallu, C. Tumoricidal and Bactericidal Properties of ZnONPs Synthesized Using *Cassia auriculata* Leaf Extract. *Biomolecules* **2020**, *10*, 982. [CrossRef]
20. Rahman, H.S.; Azizi, S.; Namvar, F.; Mohamad, R.; Rasedee, A.; Soltani, M.; Rahim, R.A. Green synthesis, characterization, and anticancer activity of hyaluronan/zinc oxide nanocomposites. *Onco Targets Ther.* **2016**, *9*, 4549–4559. [CrossRef]
21. Kumar, J.; Datt, C.; Verma, S.K.; Rani, K. Biological Role of Withania somnifera against Promiscuity of Zinc Oxide Nano Particles and Its Interaction with Macrophages. In *Biochemical Toxicology-Heavy Metals Nanomaterials*; IntechOpen: London, UK, 2020.
22. Xia, T.; Kovochich, M.; Brant, J.; Hotze, M.; Sempf, J.; Oberley, T.; Sioutas, C.; Yeh, J.I.; Wiesner, M.R.; Nel, A.E. Comparison of the Abilities of Ambient and Manufactured Nanoparticles To Induce Cellular Toxicity According to an Oxidative Stress Paradigm. *Nano Lett.* **2006**, *6*, 1794–1807. [CrossRef]
23. Song, W.; Zhang, J.; Guo, J.; Zhang, J.; Ding, F.; Li, L.; Sun, Z. Role of the dissolved zinc ion and reactive oxygen species in cytotoxici-ty of ZnO nanoparticles. *Toxicol. Lett.* **2010**, *199*, 389–397. [CrossRef] [PubMed]
24. Kumar, J.; Mitra, M.D.; Hussain, A.; Kaul, G. Exploration of immunomodulatory and protective effect of Withania somnifera on trace metal oxide (zinc oxide nanoparticles) induced toxicity in Balb/c mice. *Mol. Biol. Rep.* **2019**, *46*, 2447–2459. [CrossRef] [PubMed]